



Title	Development of a Bidirectional Pedestrian Stream Model with an Oblique Intersecting Angle
Author(s)	Xie, S; Wong, SC; Lam, WHK; Chen, A
Citation	Journal of Transportation Engineering, 2013, v. 139 n. 7, p. 678-685
Issued Date	2013
URL	http://hdl.handle.net/10722/185776
Rights	Journal of Transportation Engineering. Copyright © American Society of Civil Engineers.

1 **DEVELOPMENT OF A BI-DIRECTIONAL PEDESTRIAN STREAM**

2 **MODEL WITH OBLIQUE INTERSECTING ANGLE**

3 Siqui XIE¹; S.C. WONG, M. ASCE;² William H.K. LAM³; Anthony CHEN⁴

4

5 **Abstract**

6 This study establishes a mathematical model that can represent the conflicting effects of two
7 pedestrian streams with an oblique intersecting angle in a large crowd. In a previous study, a
8 controlled experiment in which two streams of pedestrians were asked to walk in designated
9 directions was used to model the bi-directional pedestrian stream of certain intersecting angles. In this
10 study, we revisit that problem and apply the Bayesian inference approach to calibrate an improved
11 model with the controlled experiment data. We also collected pedestrian movement data from a busy
12 crosswalk using a video observation approach. The two sets of data are used separately to calibrate
13 our proposed model. With the calibrated model, we study the relationship between speed, density, and
14 flow in both the reference and conflicting streams, and predict how these factors affect the
15 interactions of moving pedestrian streams. We find that the speed of one stream not only decreases
16 with its total density, but it also decreases with the ratio of its flow in relation to the total flow, i.e., the
17 speed of the pedestrians decreases if their stream changes from the major to the minor stream. We
18 also observe that the maximum disruption induced by pedestrian flow from an intersecting angle
19 occurs when the angle is near 135°.

¹ Student, Department of Civil Engineering, The University of Hong Kong, Pokfulam Road, Hong Kong, China
(Corresponding author). E-mail: seakay@hku.hk; Tel.: +852-2859-2662; Fax: +852-2517-0124

² Chair Professor, Department of Civil Engineering, The University of Hong Kong, Pokfulam Road, Hong Kong,
E-mail: hhecwsc@hku.hk; Tel.: +852-2859-1964; Fax: +852-2559-5337

³ Chair Professor, Department of Civil and Structural Engineering, The Hong Kong Polytechnic University,
Hung Hom, Kowloon, Hong Kong, E-mail: william.lam@polyu.edu.hk; Tel.: +852-2766-6054; Fax: +852-
2334-6389

⁴ Professor, Department of Civil and Environmental Engineering, Utah State University, Logan, UT 84322-4110,
USA, E-mail: anthony.chen@usu.edu; Tel.: +1 (435) 797-7109; Fax: +1 (435) 797-1185

20 **CE Database subject headings:** Pedestrians; Traffic surveys; Bayesian analysis; Measurement;
21 Experimentation.

22 **Keywords:** Pedestrian stream model; Bi-directional interactions; Empirical studies; Bayesian
23 inference

24

25 **Introduction**

26 Walking is an environmentally friendly mode of transportation. A good understanding of
27 pedestrian activities and the effective planning of walking facilities are particularly important for
28 densely populated Asian cities such as Hong Kong. Previous studies have used observational surveys
29 and controlled experiments to examine one-dimensional and bi-directional pedestrian streams. Video
30 recording has been a widely applied survey method in these studies, as it is economic, convenient, and
31 has relatively high accuracy. The video provides a real-time record of the pedestrian movements from
32 which it is possible to extract the position of each individual pedestrian at any moment. Bi-directional
33 pedestrian streams are more common in daily life than one-dimensional pedestrian movements, but
34 very few previous studies have modeled bi-directional streams. Hence, in this study, we video
35 recorded the pedestrian movements at a busy crosswalk in Hong Kong and extracted relevant data to
36 develop a mathematical model that reflects the relationships between macroscopic quantities related
37 to bi-directional pedestrian flow, including the speed, density, flow, and the intersecting angle
38 between the reference stream and the conflicting stream.

39 Since Hughes (2002) proposed equations governing two-dimensional pedestrian flow and pointed
40 out the importance of the conflicting effect induced by the interactions of bi-directional pedestrian
41 streams, studies have increasingly focused on bi-directional pedestrian flows. Compared to uni-
42 directional pedestrian flows, bi-directional flows are more complicated but also more commonly
43 found in various walking facilities such as crosswalks, metro stations and even shopping malls. Lam
44 et al. (2002, 2003) investigated bi-directional pedestrian movement in several walking facilities in
45 Hong Kong, including signalized crosswalks in various areas. Ye et al. (2008) conducted an

46 observational experiment on several walking facilities in Shanghai, including a two-way passageway.
47 In addition to observational surveys, controlled experiments have been widely used in the study of bi-
48 directional pedestrian behavior, as they can be designed to cover the full range of model parameters
49 and provide data under a variety of conditions.

50 However, most experimental studies on bi-directional pedestrian flows have only considered the
51 counter-flow case, in which two streams of pedestrians walk toward each other. Some experiments
52 have involved crossing flows with two perpendicular streams, such as those conducted by Daamen
53 and Hoogendoorn (2003) and Helbing et al. (2005). Moreover, Wong et al. (2010) and Ando et al.
54 (1988) looked at cases with an oblique intersecting angle between two streams of pedestrians, which
55 are situations rarely discussed in the literature.

56 Many researchers have investigated the counter-flow case using data from studies of uni-
57 directional pedestrian flows. Daamen and Hoogendoorn (2003) and Kretz et al. (2006a) also
58 performed experiments for pedestrian counter flow in corridors of various widths. Kretz et al. (2006b)
59 found that the performance of counter flow, in terms of macroscopic quantities such as passing time,
60 speed, and flux, is not necessarily lower than that of situations without counter flow. They pointed out
61 that pedestrians are able to increase their efficiency in using space to a certain degree, and thus
62 compensate for the existence of counter flow. Another interesting finding was the phenomena of lane
63 formation, whereby the pedestrians in the experiment always chose right-hand traffic. As this
64 experiment was conducted in Germany and most of the participants were German, the authors
65 suggested that it would be useful to perform similar experiments in countries with left-hand traffic, to
66 check the correlation between vehicular traffic rules and pedestrian behavior. In terms of lane-
67 formation, Helbing et al. (2005) observed similar self-organization phenomena in a series of
68 experiments for bi-directional pedestrian flows in bottlenecks with differing widths.

69 However, the pedestrian streams in these experiments were mainly opposite to each other, and
70 there was usually a 180° angle between the two streams. The investigation by Ando et al. (1988) was
71 one of the few studies on bi-directional pedestrian flow to include an oblique intersecting angle. Jiang

72 et al. (2009) proposed a reactive dynamic continuum–user equilibrium model to simulate bi-
73 directional pedestrian flows. Xiong et al. (2011) proposed a high-order computational scheme for the
74 Jiang et al. model that proved more efficient than the first-order methods. These two studies, although
75 they involved little empirical data, considered the intersecting angle between the two streams, which
76 provided useful information for further studies on the influence of intersecting angles in bi-directional
77 pedestrian flows. Recognizing the limitations of previous research on this problem, Wong et al. (2010)
78 conducted controlled experiments to address them.

79 In their controlled experiment, Wong et al. (2010) used a modified form of Drake’s model (1967)
80 for one-dimensional traffic. In that model, the density of the streams and the intersecting angle are
81 independent variables. As one of the few studies on bi-directional pedestrian streams with an oblique
82 intersecting angle, the study advanced our understanding of bi-directional pedestrian streams.
83 However, in re-evaluating the study, we found that the model could be further modified to better
84 describe the bi-directional pedestrian movements if it included a key variable.

85 This paper presents the formulation of the improved model and compares that model with the
86 original version. We also collected a new set of data at a crosswalk in Hong Kong to verify the
87 improved model. In a real-world situation, pedestrians have their own destinations rather than
88 assigned directions, and the pedestrians’ demographic composition is a better reflection of reality than
89 the student sample used in the controlled experiments. In the next section of this paper, we describe
90 the data collection in this circumstance, and then demonstrate the formulation of the improved model
91 for the bi-directional pedestrian stream. Finally, we discuss the model calibration results and the
92 properties of the improved model.

93

94 **Data**

95

96 Two sets of data were used in this study. The first was the dataset from the controlled experiment
97 performed by Wong et al. (2010), and the other was collected from an observational survey of a busy

98 signalized crosswalk in Hong Kong. Through a thorough comparison and study of these two data sets,
99 we identified a key variable that could better describe the bi-directional pedestrian movements and
100 formed the basis of formulating an improved model. The data from the controlled experiment were
101 used to recalibrate the improved model. The data from the field observation were then used to verify
102 that model in a real-world situation.

103

104 ***Controlled Experiment***

105

106 The controlled experiment was conducted in a sports stadium. Volunteer students were asked to
107 walk in designated directions, and the intersecting angles between the paths for the two streams were
108 set at 45°, 90°, 135° and 180° (Fig. 1). The total density and the spilt ratio of the pedestrian numbers
109 were controlled to test how these factors affected the speed of the pedestrian streams.

110

111 [Insert Figure 1 Here]

112

113 ***Field Observation***

114

115 A new set of data was collected so that we could apply the model to a real-world situation. The
116 site selected for video recording was the busy signalized crosswalk between Queen's Road Central
117 and D'Aguilar Street in Central District, Hong Kong. The camera was set at the top of a nearby tall
118 building, providing us with an ideal top view of the junction.

119

120 [Insert Figure 2 Here]

121

122 ***Video Data Processing***

123

124 The video was taken at 25 frames per second under a PAL analogue television encoding system.
125 The pictures, in JPEG format, were extracted from the video every 5 frames, i.e., every 0.2 s. This

126 sampling interval ensured the smooth and complete tracking of pedestrian movements for this study.
127 At the selected junction, the signal cycle was about 120 s, and there was a 15 s pedestrian phase in
128 each cycle. However, we were only interested in periods during which the two pedestrian streams
129 fully mixed, i.e., the short period, about 2 s, in the middle of each pedestrian phase. The final dataset
130 consisted of 65 cycles, with an average of 103 pedestrians in each cycle. In total, we traced the
131 movements of more than 6000 pedestrians in the video.

132

133 *Acquisition of Positions*

134

135 To obtain the image coordinate of each pedestrian in the region of interest (ROI), the selected
136 video images were imported into a specially designed Visual Basic (VB) program, and the positions
137 of pedestrians were marked manually. As shown in Fig. 3, we marked the pedestrians' heads and feet,
138 if visible, with blue and green dots, respectively. This prepared the video data for the coordinate
139 transformation necessary to obtain the real-world positions.

140

141 [Insert Figure 3 Here]

142

143 *Computation of Average Speed and Density*

144

145 As shown in Fig. 4, the distribution of pedestrians in the region was not homogeneous. To ensure
146 that the computed average speed and density reflected the true relationship between speed and density,
147 we divided the region into 18 sub-areas, each measuring 3m x 3m. The sub-areas were distributed
148 according to the size of the crosswalk, three across the Queen's Road Central, and six along the road.

149

150 [Insert Figure 4 Here]

151

152 In total, as each sub-area gave one data point, we obtained 18 data points from each frame
153 (picture) for data analysis.

154 To summarize, we counted 1160 pedestrians in the controlled experiment and 6788 in the field
155 observation. As shown in Table 1, the average speed of pedestrians in the field observation was higher
156 than in the experiment, but the average density of pedestrians in the field observation was lower than
157 in the experiment.

158

159 [Insert Table 1 Here]

160

161 **Model Formulation**

162 *Original Model*

163 The model used by Wong et al. (2010) is a modification of the one-dimensional traffic model
164 proposed by Drake et al. (1967):

$$165 \quad V_r = V_f \exp(-\theta_r(\rho_r + \rho_c)^2) \exp(-\theta_c(1 - \cos\varphi)\rho_c^2) \quad (1)$$

166 where

167 V_r is the speed of the reference stream;

168 V_f is the free-flow speed;

169 ρ_r is the density of the reference stream;

170 ρ_c is the density of the conflicting stream;

171 φ is the intersecting angle between the two streams;

172 θ_r and θ_c are parameters reflecting the sensitivity of speed to density on isotropic and conflicting
173 effects, respectively.

174

175 This model satisfies the following natural boundary conditions as stated in the original study.

176 1. When $\varphi = 0$, there is effectively only a single stream of pedestrians.

177 2. The interaction effect due to the conflicting pedestrian stream should be symmetrical across the
178 180° intersecting angle.

179 3. When the walking facility is nearly empty, the speed of the reference pedestrian stream should
180 approach the free-flow speed, i.e., $V_r \rightarrow V_f$ when $\rho_r, \rho_c \rightarrow 0$.

181 4. When the walking facility is nearly empty, the flow of the reference pedestrian stream should
182 approach zero, that is, $q_r \rightarrow 0$ when, $\rho_r, \rho_c \rightarrow 0$, because $q_r = V_r \rho_r$.

183 5. When the walking facility is nearly empty, the addition of a pedestrian in the reference or the
184 conflicting stream does not affect the speed of the reference stream, i.e., $\partial v_r / \partial \rho_r \rightarrow 0$ and
185 $\partial v_r / \partial \rho_c \rightarrow 0$, when $\rho_r, \rho_c \rightarrow 0$.

186 In this model, an exponential term is added to describe the conflicting effect from the opposite
187 stream. The conflicting effects from the opposite stream mainly depend on the density of the
188 conflicting stream, and on the intersecting angle between the two streams: i.e., the direction of the
189 opposite stream. The conflicting effect is symmetrical across 180° .

190 As the two streams are actually each other's conflicting stream, we can also represent the speed of
191 the conflicting stream as in Eq. (2):

$$192 \quad V_c = V_r \exp(-\theta_r(\rho_r + \rho_c)^2) \exp(-\theta_c(1 - \cos \varphi)\rho_r^2) \quad (2)$$

193 Dividing Eq. (1) by Eq. (2), we obtain:

$$194 \quad \frac{V_r}{V_c} = \exp(\theta_c(1 - \cos \varphi)(\rho_r^2 - \rho_c^2)) \quad (3)$$

195
$$\frac{V_r}{V_c} = \exp\left(\theta_c (1 - \cos \varphi) \left(\rho_t^2 \left(1 - \frac{2\rho_c}{\rho_t}\right)\right)\right), \quad (4)$$

196 where ρ_t represents the total density, i.e., the sum of ρ_r and ρ_c . This indicates that the ratio between the
 197 speed of the two streams is governed by the density difference between the two streams. If $\rho_r > \rho_c$,

198 i.e., $\frac{\rho_c}{\rho_t} < 0.5$, then $\frac{V_r}{V_c} > 1$. This means that the stream with a higher density will suffer a relatively

199 lower conflicting effect from the other stream, so that it can achieve a higher speed, and vice versa.

200 Both the experimental data and the field data agree with the model that $\frac{V_r}{V_c}$ is generally larger

201 than 1, when the density ratio $\frac{\rho_c}{\rho_t}$ is less than 0.5. However, as shown in Table 2, the correlation

202 between these two quantities is quite weak in both sets of data, i.e., there is no noticeable increase in
 203 the conflicting effect as the density of the conflicting stream rises. On the other hand, we find that

204 there is a much stronger correlation between the speed ratio and the flow ratio, $\frac{q_r}{q_c}$, such that the flow

205 of one stream is the product of its speed and density, i.e., $q_r = V_r \rho_r$, $q_c = V_c \rho_c$ and $q_t = q_r + q_c$.

206

207 [Insert Table 2 Here]

208

209 As shown in Table 2, the correlation between speed ratio and flow ratio is more significant. This

210 suggests that the density difference may not be a good way to represent the speed in bi-directional

211 pedestrian stream movements, as the density of one stream is a static quantity and does not reflect the

212 movement of the stream. However, the conflicting effect induced by the opposite stream is dependent

213 not only on the density of the conflicting stream itself, but also on the movements of both streams.

214 Therefore, to better model the conflicting effect between the two opposite streams, we adopt a

215 momentum term, *flow* (density \times speed, analogous to mass \times speed in a physical system), that reflects
 216 the relative movement momentum between the two streams and the density difference. This improved
 217 model is discussed in the next section.

218

219 ***Improved Model***

220

221 Our modification to the previous model is as follows:

$$222 \quad V_r = V_f \exp(-\theta(\rho_r + \rho_c)^2) \exp\left(-\beta\left(1 - \frac{V_r \rho_r}{V_r \rho_r + V_c \rho_c}\right)(1 - \cos \alpha \varphi)(\rho_r + \rho_c)\right) \quad (5)$$

$$223 \quad V_c = V_f \exp(-\theta(\rho_r + \rho_c)^2) \exp\left(-\beta\left(1 - \frac{V_c \rho_c}{V_r \rho_r + V_c \rho_c}\right)(1 - \cos \alpha \varphi)(\rho_r + \rho_c)\right) \quad (6)$$

224 where V_r , V_c , ρ_r , ρ_c and φ are defined in equation (1), θ , β and α are coefficients, and $\frac{V_r \rho_r}{V_r \rho_r + V_c \rho_c}$ is

225 the flow ratio (flow = density \cdot speed, the momentum term), with $\frac{V_r \rho_r}{V_r \rho_r + V_c \rho_c} = 1$, when both $\rho_r = 0$

226 and $\rho_c = 0$.

227 The improved model satisfies the same boundary conditions as the original model. It can also be
 228 reduced to a one-dimensional Drake model when the intersecting angle $\varphi = 0$.

229

230 ***Bayesian Inference***

231

232 Bayesian inference is a method of statistical deduction in which Bayes' theorem is used to
233 calculate how the prior distribution changes according to new evidence. This method is a modeling
234 approach for parameter estimation that integrates prior and current information. The ultimate aim of
235 Bayesian inference is to obtain the posterior distribution of all unknowns, i.e., the parameters of
236 interest.

237 To perform Bayesian inference, we used the WinBUGS software to estimate the proposed model.
238 According to Ioannis Ntzoufras (2009), Bayesian statistics regard all unknown parameters as random
239 variables, so prior distribution must be defined initially. Assuming that the prior distribution for all of
240 the parameters to be estimated is normal, the prior mean μ and variance σ^2 should be specified for
241 each parameter. When we strongly believe that the estimate mean is accurate, the variance can be set
242 relatively low and great uncertainty concerning to the prior mean can be represented by large variance.
243 No prior information is available when we first apply the proposed model to the controlled experiment
244 data. Therefore, a prior distribution that will not influence the posterior distribution should be
245 specified to let the data speaks for themselves: i.e., a non-informative prior distribution should be
246 adopted. In practice, the variance σ^2 is set very large ($\sigma^2=10000$) such that the prior distribution
247 contributes negligible information to the posterior distribution.

248 To evaluate the goodness-of-fit and to check the performance of the models, we used the deviance
249 information criterion (DIC) and the posterior p-value to assess both the statistical fit and the
250 prediction of the proposed model. The DIC is useful in Bayesian model selection as it measures how
251 well the model fits and considers penalties on number of parameters. Generally, the model with low
252 DIC value is preferred (Spiegelhalter et al., 2002). The posterior p-value checks the goodness-of-fit by
253 comparing the model's predictive data to the observed data. This assumes that if experiments with the
254 same parameters were replicated in the future we would obtain another set of observed data. If the
255 model is appropriate for the observed data, the replicated data should be very close to the observed
256 data. Hence, the difference between the two sets of data will reveal the goodness-of-fit of the model.
257 The posterior p-value is defined as the probability that the replicated data is more extreme than the

258 observed data. Therefore, the closer the posterior p -value is to 0.5, the better the fit of the model
259 (Gelman et al., 2004).

260 Besides these statistics in the Bayesian framework, we also adopted the mean absolute percentage
261 error (MAPE), the root mean square error (RMSE), and the relative root mean square error (RRMSE)
262 as statistics to evaluate the goodness-of-fit for the models.

263

264 **Results and Discussion**

265

266 Table 3 presents the calibration results of the two models for the controlled experiment data.

267

268 [Insert Table 3 Here]

269

270 In Table 3, it can be seen that the value of free-flow speed V_f is 1.074 m/s (0.95 CIs: 1.065, 1.083),
271 and the parameter of isotropic effect θ is 0.062 (0.95 CIs: 0.058, 0.066) in the improved model. These
272 values are similar to those in the original model. The calibrated value of β is 0.072 (0.95, CIs: 0.064,
273 0.080), and α is 1.271 (0.95, CIs: 1.208,1.336), which is between 1 and 2, indicating that the
274 intersecting angle between the two streams has a negative influence on speed, and this conflicting
275 effect is maximized when the intersecting angle is between 90° and 180° . The DIC value for the
276 improved model is far less than that of the original model, and the posterior p -value (the closer to 0.5,
277 the better the model fit) and other statistical indexes of the improved model also indicate that the
278 improved model results in a better fit of the experimental data.

279 There is no doubt that the controlled experiment is a very good sample of bi-directional pedestrian
280 stream movements with oblique intersecting angles. The volunteers were asked to walk in designated
281 directions, and a variety of densities and intersecting angles were tested. Hence, the data collected

282 from the controlled experiment are of good quality. However, no experiment is the same as a real-
283 world situation. The data from the observational survey are less controllable than those in the
284 experiment, as we cannot control the density of the crowds or the directions the pedestrians walk.
285 However, these data are a better reflection of reality.

286 To test the model's applicability to a real-world situation, we adopt the Bayesian method to
287 further calibrate the model with the field data collected from the observational survey. For the
288 parameters reflecting the interactions between pedestrians, θ , β , and α , we use the posterior
289 distribution from the controlled experiment to provide prior distribution, as shown in Table 4.

290

291 [Insert Table 4 Here]

292

293 However, for the free-flow speed (V_f), no prior information is available. As pedestrians in the
294 crosswalk walk much faster than the volunteers in the experiment, the free-flow speed clearly depends
295 on the environment in which the data are collected. To assess the free-flow speed, we extract the data
296 points (on the speed of the reference stream) that had low total density ($\rho_r + \rho_c < 1$) from both the
297 experiment and the field survey, and perform a t -test. We find that the means of the speed for these
298 two situations ($\rho_r + \rho_c < 1$) are significantly different (at a 0.1% level). The two means are 1.074 m/s
299 for the experiment and 1.307 m/s for the field survey. The mean value for the controlled experiment
300 (1.074 m/s) is the same as the calibrated free-flow speed shown in Table 3. The mean value for the
301 field data is 30% greater than that in the experiment. Therefore, the free-flow speed should be revised
302 for the model in accordance with the field data.

303 Finally, we calibrate the model for the field data and compare statistics to those of the controlled
304 experiment, as shown in Table 5.

305

306 [Insert Table 5 Here]

307 Table 5 shows that the free-flow speed increases to 1.326 m/s when the field data is used to
308 update the model to account for the people hurrying through the crosswalk. This free-flow speed is
309 consistent with that measured in an empirical study reported by Lam et al. (2002), which examined a
310 signalized crosswalk in Hong Kong. The posterior p -value indicates that the model generally fits the
311 field data. Although the mean absolute percentage error and the relative root mean square error have a
312 roughly 10% increase, this is still reasonable when considering the large variability of the field data
313 (standard deviation = 0.5 m/s) compared to the experimental data (standard deviation = 0.2 m/s).

314 As the model's form is a set of structural equations, it is not straightforward to compute the speed
315 of one stream with a given ρ_r and ρ_c . Therefore, Fig. 5 provides the design charts for finding the speed
316 of the reference stream that corresponds to ρ_r and ρ_c under different intersecting angles. Fig. 5 also
317 shows the relationships between the speed of the reference stream and its density, when the density of
318 the conflicting stream is kept constant. Generally, when the density of the conflicting stream is low
319 ($\rho_c < 1$), the speed of the reference stream first decreases very slightly (from 1.3 to 1.2 m/s) as the
320 density of the reference stream gradually increases from 0 to 1 ped/m², because the total density is
321 also low and the interaction between pedestrians is weak at this stage. The reference stream's speed
322 reduces more significantly as the total density builds, and the conflicting effect from the opposite
323 stream grows as the number of interactions between pedestrians increases. Finally, the decline
324 becomes stable when the reference stream's density increases to the point that it becomes the major
325 stream. In contrast, when the density of the conflicting stream is relatively high ($\rho_c > 1$), it skips the
326 first phase that was seen in the previous situation. The speed of the reference stream drops sharply at
327 the beginning, as the conflicting stream is absolutely the major stream when the reference stream has
328 very low density. Thus, the conflicting effect from the opposite stream is tremendous at the starting
329 stage. The gradient gradually reduces as the density of the reference stream increases.

330

331 [Insert Figure 5 Here]

332 Fig. 5 also shows the effects on stream speed induced by different intersecting angles. When the
333 intersecting angle increases from 0° to 90° , the pedestrians actually have the same destination, i.e., the
334 opposite side of the crosswalk, although they may enter the crosswalk area from different points. The
335 smaller the intersecting angle, the less difference there is between their directions. Hence, speed
336 reduces as angle increases. However, when the intersecting angle exceeds 90° and continues to
337 increase between 90° and 180° , the speed no longer decreases steadily with the increase of the
338 intersecting angle. The worst situation occurs when the intersecting angle is 135° . We use Fig. 6 to
339 illustrate this phenomenon. When the intersecting angle between the two streams is 90° (Fig. 6(a)),
340 each stream of pedestrians is walking orthogonally to the other, and the pedestrians can easily find
341 gaps in the conflicting stream. When the intersecting angle is 180° (Fig. 6(b)), the formation of self-
342 organized lanes helps to reduce the conflicting effect induced by the opposite stream. However, when
343 the intersecting angle is 135° (Fig. 6(c)), there is no obvious gap in the conflicting stream, and
344 individual pedestrians must zigzag to avoid others coming the other way. Such interactions between
345 pedestrians of different streams reduce their walking speeds.

346 To illustrate this flow-density relationship, a straightforward comparison between situations with
347 different intersecting angles is shown in Fig. 7. Fig. 7 also shows that the optimum total density under
348 different intersecting angles is about $2.0 \sim 3.0 \text{ ped/m}^2$, with a maximum flow of about $1.8 \sim 2.1$
349 ped/m/s (for different intersecting angles). This value is slightly higher than the value reported in
350 Wong et al. (2010). It is not surprising that pedestrians walk through a crosswalk faster than students
351 cross a sports stadium in an experiment.

352

353 **Conclusions**

354 Expanding on Drake's model, we developed a mathematical model to represent the movements of
355 bi-directional pedestrian flows, which introduces the flow ratio and the intersecting angle as attributes

356 that influence the speed of the streams. Two sets of data were collected, one from a controlled
357 experiment and the other from an observational survey. Bayesian inference was adopted in the
358 parameter calibration. The empirical data was used to calibrate the model as it completely and
359 homogeneously covers the different possible intersecting angles and the different levels of flows. The
360 calibrated parameters of the controlled experiment were used as the prior data in the substantial
361 calibration of the field data. The field data was then used to update the model to reflect real-world
362 situations.

363 Compared to the previous model, the new model achieves a better fit for experimental data, and
364 continues to satisfy the same boundary conditions as the original model. The updating process with
365 the field data also improves the model to reflect real-world situations. The new model reflects the
366 reality that the speed of the streams in bi-directional pedestrian movements depends not only on the
367 density of each stream, but also on the factors of the flow speed in both streams and the intersecting
368 angle between the two streams. Therefore, the new model is more comprehensive in representing the
369 interactions of bi-directional pedestrian flows. Finally, the new model also shows that the conflicting
370 effect induced by the intersecting angle maximizes when the angle is near 135° . At this angle,
371 pedestrians must pay more attention to avoid pedestrians in the conflicting flow, as there is neither
372 lane formation nor a straightforward gap between streams in such situations.

373 These findings build on previous controlled experiments that focused on bi-directional pedestrian
374 streams with oblique intersecting angles. Data on the flows of streams are added to data from the
375 previous experiments to better describe the movements and interactions of flows. The result is an
376 improved form of model for bi-directional pedestrian flows. The use of on-site observation helps us to
377 better understand the difference between experimental and real situations, and this improves the
378 model. The results are consistent with similar observations by other researchers. However, more
379 observational surveys on different walking facilities should be conducted to make the model even
380 more congruent with actual pedestrian behavior. Once we have a comprehensive understanding of bi-
381 directional pedestrian flows, we can further extend the study to multi-directional pedestrian flows, in
382 which the interactions between streams can be quite different from the bi-directional ones.

383

384 [Insert Figure 6 Here]

385

386 [Insert Figure 7 Here]

387

388 **Acknowledgements**

389 The work described in this paper was supported by a Research Postgraduate Studentship and a
390 grant from the Research Grants Council of the Hong Kong Special Administrative Region, China
391 (Project No. HKU 7184/10E).

392

393 **References**

394 Ando, K., Ota, H. and Oki, T. (1988). "Forecasting the flow of people." *Railway Research Review*,
395 45(8), 8-14 (in Japanese).

396 Daamen, W. and Hoogendoorn, S. P. (2003). "Experimental research of pedestrian walking behavior."
397 *Transportation Research Record*, 1828, 20-30.

398 Drake, J., Schofer, J. and May, A. 1967. "A statistical analysis of speed density hypotheses." In
399 *Proceedings of the Third International Symposium on the Theory of Traffic Flow*. New York:
400 Elsevier.

401 Fung, G. S. K., Yung, N. H. C. and Pang, G. K. H. (2003). "Camera calibration from road lane
402 markings." *Optical Engineering*, 42(10), 2967-2977.

403 Gelman, A. (2004). *Bayesian Data Analysis*. Boca Raton, FL, Chapman & Hall/CRC.

404 He, X. C. and Yung, N. H. C. (2007). "New method for overcoming ill-conditioning in vanishing-
405 point-based camera calibration." *Optical Engineering*, 46(3), 037202.

406 Helbing, D., Buzna, L., Johansson, A. and Werner, T. (2005). "Self-organized pedestrian crowd
407 dynamics: Experiments, simulations, and design solutions." *Transportation Science*, 39, 1-24.

408 Hoogendoorn, S. P. and Daamen W. (2005). "Pedestrian behavior at bottlenecks." *Transportation*
409 *Science*, 39(2), 147-159.

410 Hughes, R. L. (2000). "The flow of large crowds of pedestrians." *Mathematics and Computers in*
411 *Simulation*, 53(4-6), 367-370.

412 Hughes, R. L. (2002). "A continuum theory for the flow of pedestrians." *Transportation Research*
413 *Part B*, 36(6), 507-535.

414 Jiang, Y., Xiong, T., Wong, S. C., Shu, C. W., Zhang, M., Zhang, P. and Lam, W. H. K. (2009) "A
415 reactive dynamic continuum user equilibrium model for bi-directional pedestrian flows." *Acta*
416 *Mathematica Scientia*, 29(6), (November 2009), 1541-1555.

417 Kretz, T., Grunebohm, A., Kaufman, M., Mazur, F. and Schreckenberg, M. (2006a). "Experimental
418 study of pedestrian counterflow in a corridor." *Journal of Statistical Mechanics-Theory and*
419 *Experiment*, P10001.

420 Kretz, T., Grunebohm, A. and Schreckenberg, M. (2006b). "Experimental study of pedestrian flow
421 through a bottleneck." *Journal of Statistical Mechanics-Theory and Experiment*, P10014.

422 Lam, W. H. K., Lee, J. Y. S., Chan, K. S. and Goh, P. K. (2003). "A generalised function for modeling
423 bi-directional flow effects on indoor walkways in Hong Kong." *Transportation Research, Part A*,
424 37(9), 789-810.

425 Lam, W. H. K., Lee, J. Y. S. and Cheung, C. Y. (2002). "A study of the bi-directional pedestrian flow
426 characteristics at Hong Kong signalized crosswalk facilities." *Transportation*, 29(2), 169-192.

427 Ntzoufras, I. (2009). *Bayesian Modeling Using WinBUGS*, Hoboken, NJ: Wiley.

428 Seyfried, A., Passon, O., Steffen, B., Boltes, M., Rupperecht, T. and Klingsch, W. (2009). "New
429 insights into pedestrian flow through bottlenecks." *Transportation Science*, 43, 395-406.

430 Seyfried, A., Steffen, B., Winkens, A., Rupperecht, T., Boltes, M. and Klingsch, W. (2009). "Empirical
431 data for pedestrian flow through bottlenecks." *Traffic and Granular Flow '07*, 189-199.

432 Spiegelhalter, D. J., Best, N. G., Carlin, B. P. and van der Linde, A. (2002). "Bayesian measures of
433 model complexity and fit." *Journal of the Royal Statistical Society, Series B (Statistical*
434 *Methodology)*, 64(4), 583-639.

435 Wong, S. C., Leung, W. L., Chan, S. H., Lam, W. H. K., Yung, N. H. C., Liu, C. Y. and Zhang, P.
436 (2010). "Bidirectional pedestrian stream model with oblique intersecting angle." *Journal of*
437 *Transportation Engineering-ASCE*, 136(3), 234-242.

438 Xiong, T., Zhang, M., Shu, C. W., Wong, S. C. and Zhang, P. (2011). "High-order computational
439 scheme for a dynamic continuum model for bi-directional pedestrian flows." *Computer-Aided*
440 *Civil and Infrastructure Engineering*, 26(4), 298-310.

441 Ye, J. H., Chen, X., Yang, C. and Wu, J. (2008). "Walking behavior and pedestrian flow
442 characteristics for different types of walking facilities." *Transportation Research Record*, 2048,
443 43-51.

444
445
446
447
448
449
450
451
452
453
454
455
456
457
458
459
460
461
462
463
464
465
466
467
468
469
470

LIST OF FIGURE AND TABLE CAPTIONS

- Figure 1. (a) Intersecting angle = 90°; (b) Intersecting angle = 135°
- Figure 2. Location of the selected site
- Figure 3. The interface of the VB program for acquisition of the coordinates
- Figure 4. Distribution of pedestrians in the region
- Figure 5. Relationship between the speed of the reference stream and the density of the reference stream at different intersecting angles: (a) 45 degrees, (b) 90 degrees, (c) 135 degrees, and (d) 180 degrees
- Figure 6. Illustration of conflicting streams with different intersecting angles (a) 90 degrees, (b) 180 degrees, and (c) 135 degrees
- Figure 7. Flow-Total density relationship under different intersecting angles ($\rho_r = \rho_c$)
- Table 1. Summary of data
- Table 2. Comparison of experimental data and field data
- Table 3. Comparison of original and improved models
- Table 4. Informative prior distribution for parameters to be estimated
- Table 5 Comparison of statistics

471 **Table 1** Summary of data

Dataset	Controlled Experiment	Field Observations
Total Pedestrian No.	1160	6788
Average Speed (m/s)	0.74	1.15
Standard Deviation of Speed (m/s)	0.2	0.5
Average Density (ped/m ²)	2.07	0.63
Standard Deviation of Density (ped/m ²)	0.51	0.33

472

473 **Table 2** Comparison between experimental data and field data

$\frac{V_r}{V_c}$	Controlled Experiment Data	Field Data
Maximum	2.46	8.01
Minimum	0.61	0.11
Mean	1.16	1.10
Standard Deviation	0.28	0.62
Correlation between $\frac{V_r}{V_c}$ & $\frac{\rho_c}{\rho_t}$	-0.099	0.038
Correlation between $\frac{V_r}{V_c}$ & $\frac{q_c}{q_t}$	-0.368	-0.331

474

Table 3 Comparison of the original and improved models

Controlled Experiment									
	Original Model					Improved Model			
Sample Size	5487					3459			
	Estimate		(95% BCIs)			Estimate		(95% BCIs)	
Calibrated Parameters	V_f	1.076	1.067	1.085		V_f	1.074	1.065	1.083
	θ_r	0.079	0.075	0.082		θ	0.062	0.058	0.066
	θ_c	0.025	0.019	0.031		β	0.072	0.064	0.080
						α	1.271	1.208	1.336
DIC	-4520.32					-7754.05			
Posterior p-value	0.5275					0.5110			
MAPE	17.7%					17.4%			
RMSE	0.1703 m/s					0.1686 m/s			
RRMSE	19.1%					18.9%			

477

Table 4 Informative prior distribution for parameters to be estimated

	Mean	Standard Deviation
θ	0.062	2.18×10^{-03}
β	0.072	4.27×10^{-03}
α	1.271	0.032

478

Table 5 Comparison of statistics

		Controlled Experiment			Field Observation		
Sample Size		3459			1737		
		Estimate	(95% BCIs)		Estimate	(95% BCIs)	
Calibrated Parameters	V_f	1.074	1.065	1.083	1.326	1.312	1.341
	θ	0.062	0.058	0.066	0.065	0.061	0.069
	β	0.072	0.064	0.080	0.078	0.070	0.086
	α	1.271	1.208	1.336	1.214	1.149	1.275
Posterior p -value		0.5110			0.5028		
MAPE		17.7%			28.8%		
RMSE		0.1703 m/s			0.3400 m/s		
RRMSE		19.1%			30.9%		



482 **Fig. 1** (a) Intersecting Angle = 90° ; (b) Intersecting Angle = 135°

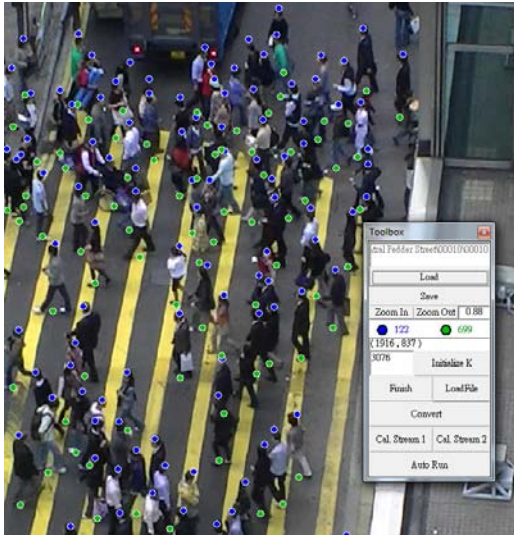
483



484

485 **Fig.2** Location of the selected site

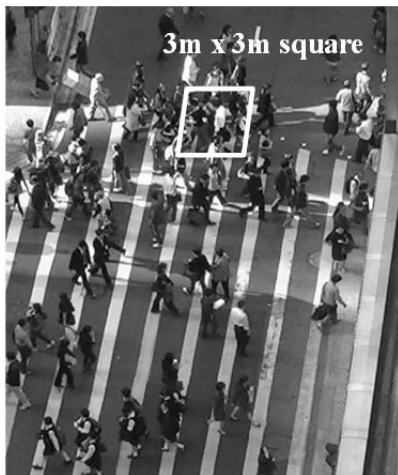
486



487

488 **Fig. 3** The interface of the VB program for acquisition of the coordinates

489

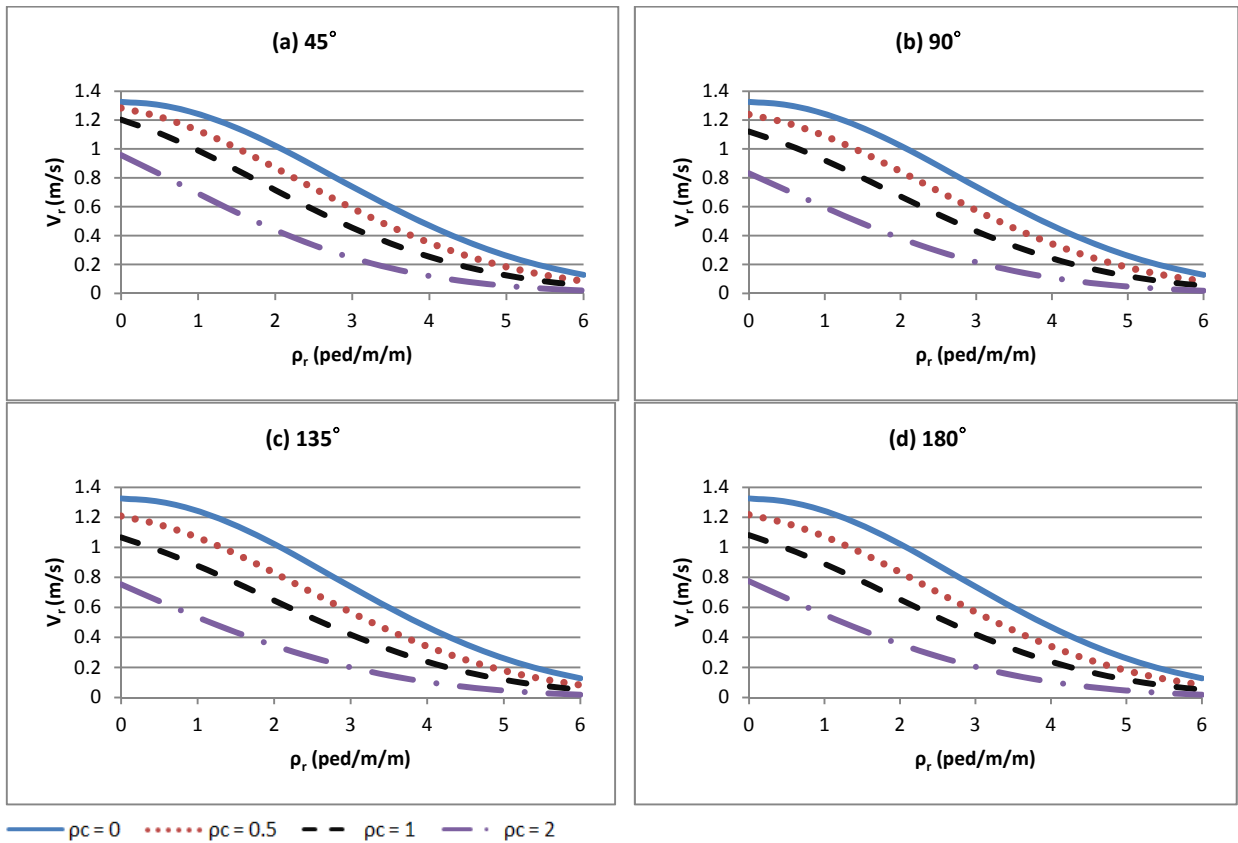


490

491 **Fig. 4** Distribution of pedestrians in the region

492

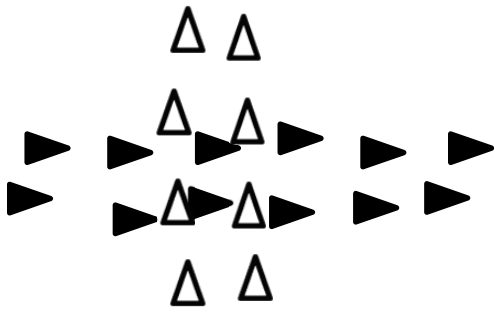
493
494



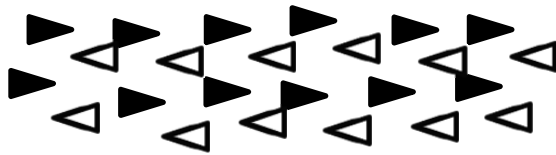
495
496
497
498
499

Fig. 5 Relationship between the speed of the reference stream and the density of the reference stream at different intersecting angles: (a) 45 degree, (b) 90 degree, (c) 135 degree, and (d) 180 degree

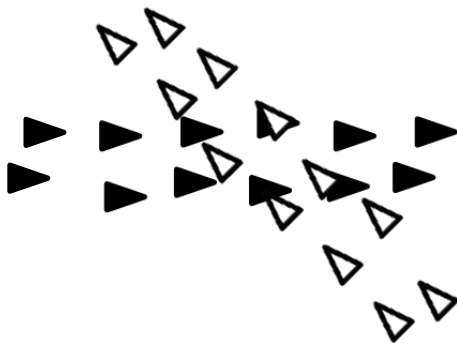
(a) 90°



(b) 180°



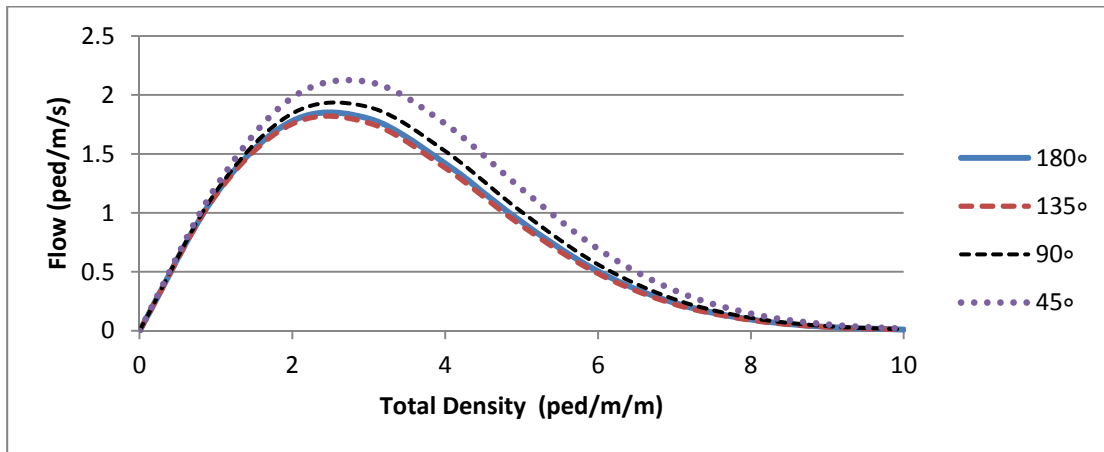
(c) 135°



500 **Fig. 6** Illustration of conflicting with different intersecting angle

501

502



503

504 **Fig. 7** Flow-Total Density relationship under different intersecting angles ($\rho_r = \rho_c$)

505

506